Journal of Hydrology: Regional Studies 24 (2019) 100607

Contents lists available at ScienceDirect

Journal of Hydrology: Regional Studies

journal homepage: www.elsevier.com/locate/ejrh

Assessment and validation of total water storage in the Chesapeake Bay watershed using GRACE

Venkataramana Sridhar[a,*], Syed Azhar Ali[a], Venkataraman Lakshmi[b]

[a] Department of Biological Systems Engineering, Virginia Polytechnic Institute and State University, VA, USA
[b] Engineering Systems and Environment, University of Virginia Charlottesville VA 22904

ARTICLE INFO

Keywords:
Water availability
Remote sensing
Hydrological modeling
Chesapeake Bay Watershed

ABSTRACT

The Chesapeake Bay is the largest estuary in the United States, and its catchment has heterogeneous hydrological and geomorphologic characteristics. It includes seven major river basins: James, Patuxent, Potomac, Rappahannock, Susquehanna, Western Shore, Eastern Shore, and York. Remote sensing data, along with in-situ observations of streamflow and simulated water budget components, can provide significant understanding of variability in water resources availability in this diverse watershed. In this study, we quantify the terrestrial water storage using both remote sensing and in-situ data and hydrologic model outputs in the Chesapeake Bay watershed. Total water storage change (TWSC) was calculated based on the combination of three methods to identify the best approach in estimating TWSC. These methods evaluated different sources of data, including Parameter elevation Regression on Independent Slopes Model (PRISM) precipitation, MODIS ET, U.S. Geological Survey observed streamflow, and the Variable Infiltration Capacity (VIC) model. Estimated TWSC were in close agreement with GRACE-derived TWSC when we employed VIC-simulated streamflow after calibration with observed streamflow. However, the use of VIC-simulated ET or MODIS-derived ET yielded similar results for TWSC. Assessment of TWSC during extreme events (drought) during the summer months revealed that predicting ET is critical for TWSC in June–August and that VIC-simulated TWSC could be a reliable proxy for GRACE data to assess the water availability in the watershed.

1. Introduction

Terrestrial water storage (TWS) is the sum of the water budget components, namely soil moisture, groundwater, snow, ice, lakes, and rivers (Rodell and Famiglietti, 2001). Generally, the water budget integrates coupled land and atmospheric processes, quantifying precipitation, evapotranspiration, and runoff to arrive at the estimates of terrestrial water storage change (TWSC) over time and space. The response of a watershed is assessed using streamflow records that reliably illustrate the space-time convolution of the watershed (Seong and Sridhar, 2017; Seong et al., 2017). However, the data for other water balance components are critical to understand extreme events such as drought, quantify return periods, and develop watershed management strategies (Lakshmi, 2016; Thilakarathne and Sridhar, 2017). Limitations in the spatial coverage of water budget components pose problems in representing the heterogeneity of the watershed at various spatial scales (Roads et al., 2003; Pan and Wood, 2006). Although the *in-situ* evapotranspiration measurements are useful for calibration or assimilation procedures, interpolation and extrapolation of these estimates are routinely done with the aid of analytical and modeling tools. These methods/tools generate some uncertainty in the estimation of

* Corresponding Author.
E-mail address: vsri@vt.edu (V. Sridhar).

https://doi.org/10.1016/j.ejrh.2019.100607
Received 4 December 2018; Received in revised form 11 March 2019; Accepted 22 May 2019

evapotranspiration, which in turn affects the computation of TWSC (Gao et al., 2010; Billah et al., 2015; Lakshmi, 2016). As the single most influential variable, precipitation is extremely important because it captures the spatial heterogeneity of the watershed (Syed et al., 2004). A distributed precipitation estimate that is based on a dense network of *in-situ* measurements is more reliable than evapotranspiration and terrestrial water storage estimates (Gao et al., 2010).

Hydrologic models that deal with land surface interactions, such as the Variable Infiltration Capacity (VIC) model, are often used to compute the terrestrial water budget (Berbery et al., 2003; Luo et al., 2005; Su and Lettenmaier, 2009; Billah and Goodall, 2011; Hoekema and Sridhar, 2013; Billah et al., 2015). These models apply water and energy balance approaches for estimating the spatial distribution of water and energy fluxes from regional to continental scales. Despite this advancement in modeling, high-resolution input data for these models are unable to account for anthropogenic effects on the hydrologic cycle (Nilsson et al., 2005; Oki and Kanae, 2006; Sridhar, 2013). The role of human disturbances that alter the basin hydrological cycle can be assessed by integrating remote sensing and in-situ data with hydrologic simulation experiments (Hanasaki et al., 2006; Haddleland et al., 2007).

Due to rapid advancements made over the past decade in acquiring high-resolution, application-specific remote sensing observations, the monitoring of hydrologic systems over vast areas where observed data are sparse has truly progressed (Tang et al., 2009; Dubayah et al., 2000; Rango and Shalaby, 1998; Schultz, 1988; Tang et al., 2009; Wagner et al., 2009). Application of satellite data in hydrologic systems analysis is also constantly evolving at relevant spatio-temporal scales (Rodell et al., 2004; McCabe et al., 2008; Sheffield et al., 2009; Tang et al., 2010; Sridhar et al., 2013). However, the use of remote sensing data for hydrologic assessments has not reached its full potential due to the inconsistent resolution of data input, interpretation and application across various spatial scales. The application of remote sensing in combination with *in-situ* observations and models can overcome these uncertainties (Sridhar et al., 2006; Sridhar and Wedin, 2009). The objective of this study is to estimate the terrestrial water storage using remote sensing and *in-situ* data with various combinations of forcing and hydrologic model outputs to evaluate the best approach for estimating the water budget at regional scales.

This work is similar in some ways to a previous study conducted by Billah et al. (2015). In that study, the researchers used GRACE (Gravity Recovery and Climate Experiment), MODIS (MODerate-resolution Imaging Spectroradiometer), NLDAS (North American Land Data Assimilation System), PRISM (Parameter elevation Regression on Independent Slopes Model), and SCAN (Soil Climate Analysis Network) data to study the space-time variability of the water balance components of the South Carolina watersheds. However, there are differences between these two studies. The 2015 study was carried out over a smaller region in South Carolina, whereas the present study of the Chesapeake Bay Watershed (CBW) spans the mid-Atlantic region of New York, Pennsylvania, Delaware, Maryland, Virginia, West Virginia and all of Washington, D.C. The main difference between the two studies is the hydrologic component being analyzed. In the 2015 study, it was evapotranspiration during 2003–2007 period, whereas in this work, we performed the simulation for TWSC from 2003 to 2016. Lastly, because the CBW is located in the densely-populated eastern region of the US, which has more than 18 million inhabitants, periodical assessments using advanced models and datasets to understand both water quantity and quality are critical for watershed, fishery and coastal ecosystem management. Based on temperature analysis of the years between 1950 and1999, an upward trend of 0.023 °C/decade was detected in the observed annual mean values in the watershed. In a changing climate, the average annual temperature is projected to increase between 1–2 °C and 1–2.5 °C between 2020–2039 relative to the baseline period under the Representative Concentration Pathways (RCP) 4.5 and RCP 8.5 scenarios. The increases were higher by the end of the 21st century (2070–2099) with 2–3.5 °C and 3–6 °C, respectively. An analysis of observed participation records for the period 1950–1999 shows that the basin experienced an increase in magnitude of 18 mm/decade. Generally, wetter conditions were projected due to climate change — i.e., more precipitation in the future when compared with the baseline period (1970–1999) for both RCP4.5 and RCP8.5 scenarios. Most of the models projected a decrease in precipitation of up to -5%, while a few projected an increase of up to 20% in mean annual precipitation (Seong and Sridhar, 2017). This study also used United States Geological Survey (USGS) gauge-station data from 19 locations to calibrate the simulated streamflow and enhance its performance, compared to the data from 2 gauge stations used in Billah et al. (2015) (USGS, 2016).

The organization of the paper is as follows: Section 2 describes the methodology adopted for the analysis, along with the study area and the various combinations of data used. Section 3 provides the results of the analysis and discussion. The summary and conclusions of the study are presented in section 4.

2. Methodology

2.1. Study area

The Chesapeake Bay is the largest estuary in the US, spanning from the Delmarva Peninsula in the east to Southwest Virginia in the west. The Fall Line divides the watershed by distinguishing heterogeneity in the basin hydrology and geomorphologic characteristics across the line. The watershed has a drainage area of 64,299 square miles, and more than 150 major rivers and streams flow through it into the North Atlantic Ocean. The watershed consists of seven major river basins: Susquehanna, Potomac, Patuxent, Eastern Shore, Western Shore Rappahannock, York and James (USEPA, 2010) in the states of Virginia, West Virginia, Delaware, Maryland, Pennsylvania, the District of Columbia and New York. The geographical location and the topography of the Chesapeake Bay are shown in Fig. 1, as are the seven major sub-basins and the stream network considered in this analysis. The northwestern region of the watershed includes the Appalachian Mountains, which have elevations up to 2000 m, while the southeastern region is marked by the presence of low-lying coastal plains. The majority of the land in the watershed is covered with forests (70%), while the remaining areas are used for agriculture (23%) and urban development (6%) (Seong and Sridhar, 2017, Kang and Sridhar, 2018). The region experiences a cooler climate, with a mean annual temperature of 10.75 °C and mean annual precipitation of 1073 mm (Kang

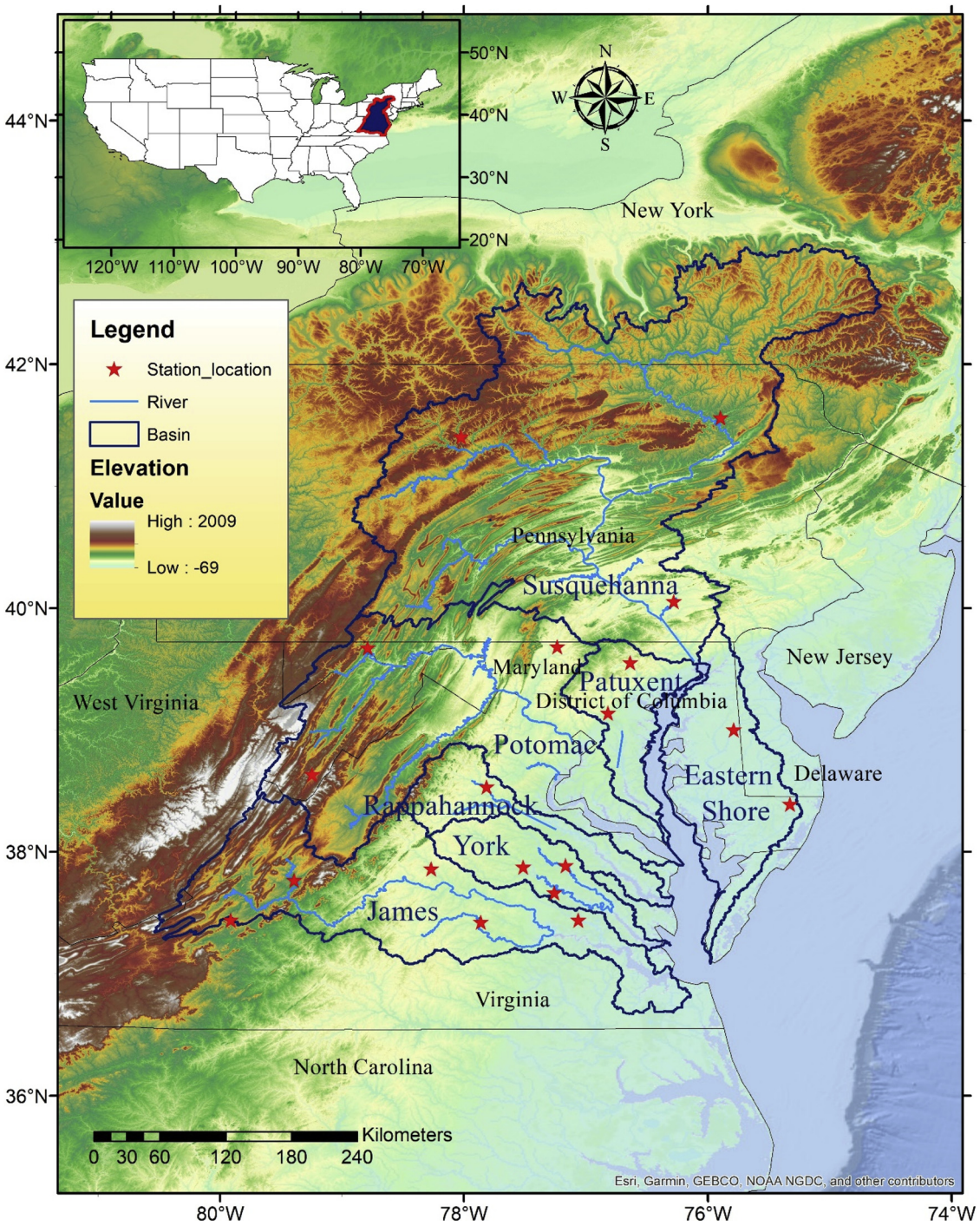

Fig. 1. Location of the Chesapeake Bay with DEM and boundaries of 7 sub-basins. Red stars indicate U.S. Geological Survey (USGS) stream gauge stations. DC, District of Columbia; DE, Delaware; MD, Maryland; NY, New York; PA, Pennsylvania; VA, Virginia; WV, West Virginia.

and Sridhar, 2018).

2.2. Estimation of water budget

The methodology for the analysis is based on the computation of TWSC using the water budget framework for the study area. Water budget accounting typically describes the partitioning of water entering and departing the top few meters of the soil column. The mass conservation equation for estimating the change in storage is:

Table 1a
Description of the precipitation, evapotranspiration and runoff data used in Methods 1, 2, and 3.

S No.	Precipitation	Evapotranspiration	Runoff
Method 1	PRISM	VIC-simulated	VIC-simulated
Method 2	PRISM	MODIS	VIC-simulated
Method 3	PRISM	MODIS	USGS streamflow

$$\frac{dS}{dt} = TWSE = \text{P-ET}+R_{in} - R_{out} \quad (1)$$

Where dS/dt or TWSC is change in terrestrial water storage, P is precipitation, ET is evapotranspiration, and R_{in} is runoff entering and R_{out} is runoff exiting the study area. In Eq. (1), the contribution of the groundwater flux to the TWSC was assumed to be negligible. Since the primary components of TWSC are precipitation, evapotranspiration and runoff, variations in each of the components will dynamically impact TWSC. We used the modeled and remotely-sensed products of these components to calculate TWSC and compared our results with the GRACE-derived TWSC.

2.3. Terrestrial water storage change estimations

In this analysis, we have used PRISM (Daly et al., 1994; Gibson et al., 2002) precipitation, two sources of evapotranspiration (VIC-simulated and MODIS) (Mu et al., 2011), and two sources of runoff data (VIC-simulated and USGS) for the estimation of TWSC. PRISM precipitation and USGS streamflow data are considered as observed, MODIS evapotranspiration is a remotely-sensed product, and simulated evapotranspiration and runoff are treated as VIC-derived model output at a monthly temporal resolution for the period from 2003 to 2016. TWSC estimates were computed for the combination of each of these products to evaluate the role of remotely-sensed and observed data in improving TWSC, and to identify the best combination of data while validating them with the GRACE-derived TWSC data. Therefore, three combination approaches were employed to derive TWSC in non-traditional ways: (1) PRISM precipitation, VIC-simulated ET, and VIC-simulated runoff; (2) PRISM precipitation, MODIS ET, and VIC-simulated runoff; and (3) PRISM precipitation, MODIS ET, and USGS runoff (Table 1a). ET alone caused significant uncertainties in flows, and therefore in estimating the TWSC. Since USGS flow data was used for calibration, use of USGS flows in combination with VIC-simulated ET became redundant. Furthermore, the focus was on obtaining a realistic estimate of the TWSC in the watershed. The effect of flows from USGS or the model was integrated adequately for this purpose.

2.3.1. Observed and remote sensing data: Precipitation

Table 1b provides the details of the data types, resolution and sources used for this study. The PRISM database (Gibson et al., 2002) for the period between 2003 and 2016 was used for precipitation. Precipitation includes liquid rain, snow, freezing rain, hail, frost, or dew. The study area primarily received liquid rain during the study period, with occasional snow or freezing rain. The 4-km PRISM data was re-gridded to 1/16-degree resolution to be used as an input to the VIC model. PRISM data is widely used for hydrologic modeling and forecasting (Schaake et al., 2004), trend analysis (Small et al., 2006), and calculation of glacier runoff (Neal et al., 2010).

Fig. 2(a) shows the spatial distribution of the mean annual precipitation (mm) in the Chesapeake Bay watershed between 2003 and 2016. The eastern region of the watershed receives high precipitation ranging from 1100 mm to 1400 mm, while the western part gets lesser precipitation of about 700 mm to 1100 mm. The mean monthly precipitation (mm/month) in the 7 sub-basins between 2003 and 2016, exhibited seasonal variations, as shown in Fig. 2 (b–h). Precipitation patterns in the sub-basins were similar pattern to the Chesapeake Bay watershed, except in the James, Eastern Shore and Patuxent basins, where there were some spikes in early Fall. The seasonal cycle of the precipitation for the Chesapeake Bay can be divided into three sets of months, with highest precipitation between May and September. Precipitation decreased from September to February, reaching its lowest magnitude in the latter month. The period from February to May was marked by a gradual increase in precipitation across the entire region.

Table 1b
Data types, resolutions and sources.

Data	Resolution	Agency	Reference
Precipitation	4 km	PRISM (Parameter elevation Regression on Independent Slopes Model)	http://prism.oregonstate.edu/
Terrestrial Water Storage Anomaly	1 degree	GRACE (Gravity Recovery and Climate Experiment)	https://grace.jpl.nasa.gov/mission/grace/
Evapotranspiration	1 km	MODIS (MODerate-resolution Imaging Spectroradiometer)	https://www.ntsg.umt.edu/project/modis/mod16.php
Streamflow	19 gauge stations	USGS (United States Geological Survey)	https://waterdata.usgs.gov/nwis/rt

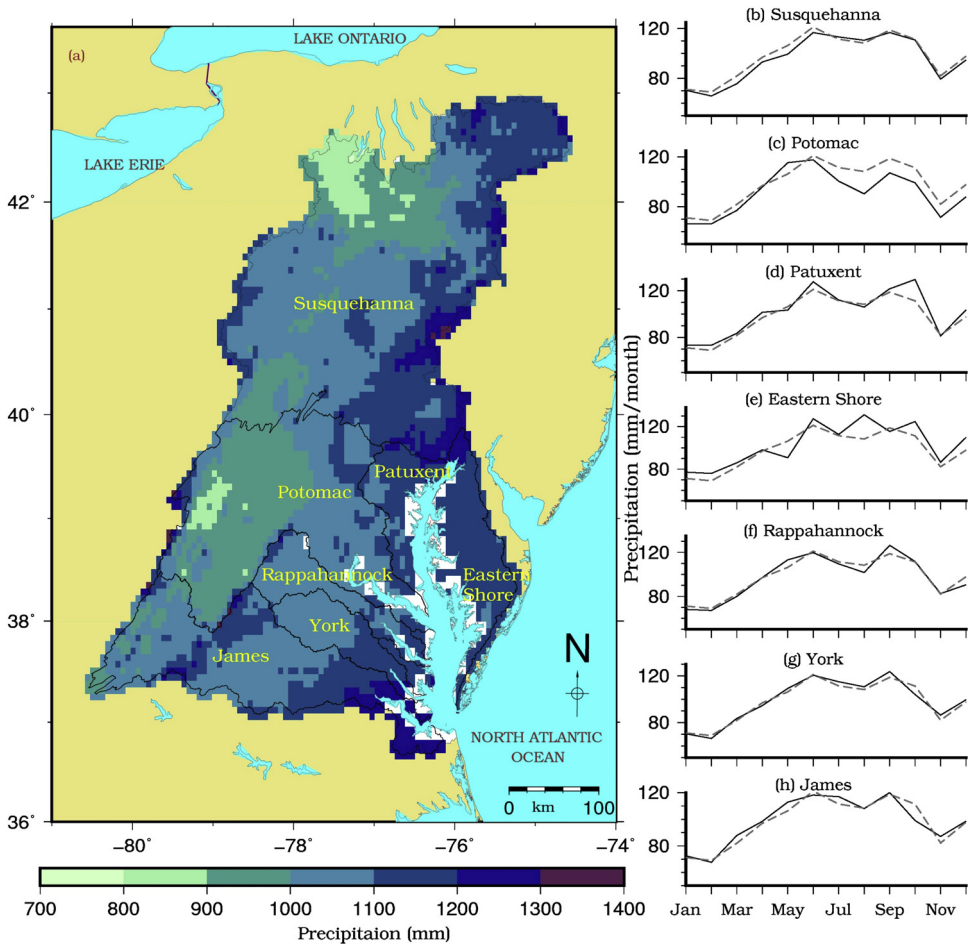

Fig. 2. (a) Mean annual precipitation (mm) of the Chesapeake Bay for 2003–2016. Mean monthly precipitation (mm/month) for 7 sub-basins (continuous black line): (b) Susquehanna, (c) Potomac, (d) Patuxent, (e) Eastern Shore, (f) Rappahannock, (g) York, and (h) James with mean monthly precipitation for Chesapeake Bay (dashed gray line).

2.3.2. Evapotranspiration

Remote sensing-based ET estimates were obtained from MODIS, based on the algorithm used by Mu et al. (2011). This approach, shown in Mu et al. (2007), adopts the Penman–Monteith ET method and combines both meteorological observations (air pressure, minimum air temperature, humidity, and radiation) and remote sensing data (land cover, albedo, LAI, and EVI) at a spatial resolution of 1 km. Mu et al. (2011) showed improvements to the estimates of nighttime and wet surface ET, soil heat flux, canopy transpiration. We used the MODIS16-derived monthly ET at a 1-km spatial resolution for the study period between 2003 and 2016 (Fig. 3), which was re-gridded to 1/16th of a degree (approximately 7 km).

2.3.3. Streamflow

The USGS-observed monthly streamflow data for the period between 1991 and 2010, available from 19 stations distributed across the watershed, were used. The geographical locations and the details of these gauge station are included in Fig. 1 and Table 2, respectively. The management in the uplands of the catchment played a critical role in the selection of these streamflow stations. We have chosen these stations in order to evaluate the basin flow under natural conditions. Farther downstream, the flow was either managed using dams and reservoirs or influenced by tides. The long-term data available for the chosen sites was also a reason to include them in our analysis. Because they are a significant component in the estimation of TWSC, the calibration and evaluation of the hydrologic model using these streamflow records were considered important for the study, and the results of those processes are shown in Fig. 4.

2.3.4. GRACE

To evaluate the storage in the watershed, Terrestrial Water Storage Anomaly (TWSA) was computed from the GRACE dataset for the period between 2003 and 2016. Monthly estimates of the gravity field data from GRACE were interpreted to estimate the water storage (Swenson and Wahr, 2006). The GRACE product available at 1-degree spatial resolution from the Jet Propulsion Laboratory

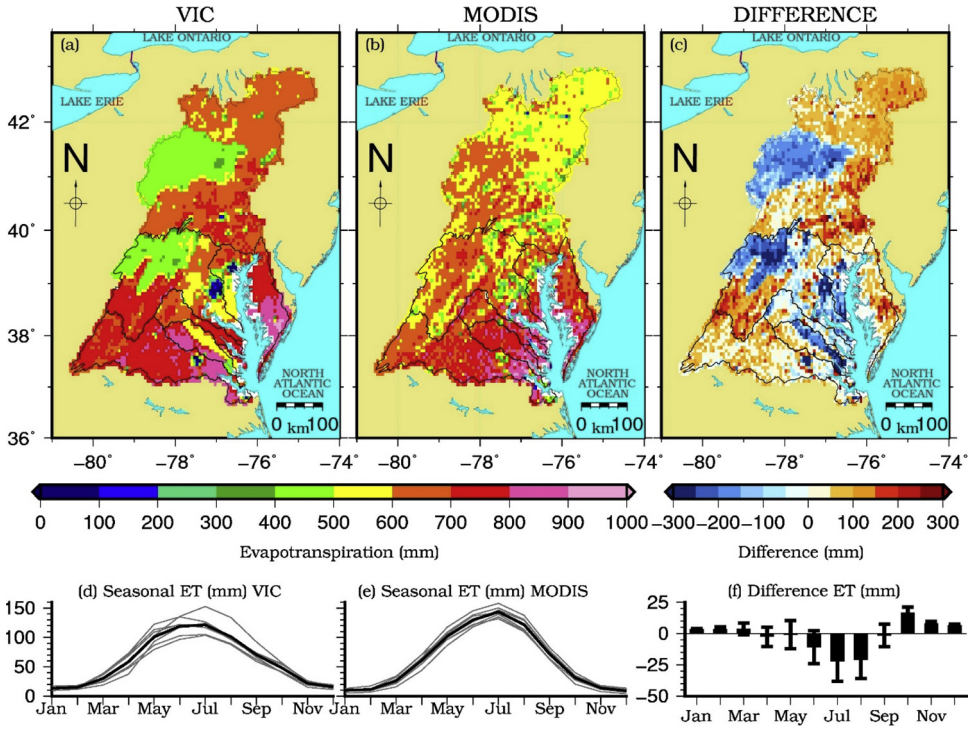

Fig. 3. Comparison between VIC-simulated and MODIS evapotranspiration from 2003 to 2016. (a) Mean annual evapotranspiration (mm) from VIC model, (b) annual evapotranspiration (mm) from MODIS, (c) Difference (VIC minus MODIS) between VIC-simulated and MODIS evapotranspiration (mm). Seasonal variation of evapotranspiration (mm/month) for VIC-modelled (d), and MODIS (e) for 7 sub-basins (gray line) and Chesapeake Bay (black line). (f) Monthly difference between VIC-simulated and MODIS evapotranspiration with uncertainty (± 1 standard deviation).

Table 2
Description of the USGS Stream Gauge station.

S. No.	USGS station	Station Name	Latitude	Longitude	Location
1	USGS02042500	Chickahominy River near Providence Forge	37°26'10″	77°03'40″	James River
2	USGS02034000	Rivanna River at Palmyra	37°51'28″	78°15'58″	James River
3	USGS02024000	Maury River near Buena Vista	37°45'45″	79°23'30″	James River
4	USGS02018000	Craig Creek at Parr	37°39'57″	79°54'42″	James River
5	USGS02040000	Appomattox River at Mattoax	37°25'17″	77°51'33″	James River
6	USGS01664000	Rappahannock River at Remington	38°31'50″	77°48'50″	Rappahannock River
7	USGS01674500	Mattaponi River near Beulahville	37°53'02″	77°09'55″	York River
8	USGS01671100	Little River near Doswell	37°52'21″	77°30'48″	York River
9	USGS01673550	Totopotomoy Creek near Studley	37°39'45″	77°15'29″	York River
10	USGS01576500	Conestoga River at Lancaster	40°03'00″	76°16'39″	Susquehanna River
11	USGS01534000	Tunkhannock Creek near Tunkhannock	41°33'30″	75°53'42″	Susquehanna River
12	USGS01544000	First Fork Sinnemahoning Cr near Sinnemahoning	41°24'06″	78°01'28″	Susquehanna River
13	USGS01639000	Monocacy River at Bridgeport	39°40'45″	77°14'04″	Potomac River
14	USGS01601500	Wills Creek near Cumberland	39°40'11″	78°47'17″	Potomac River
15	USGS01627500	South River at Harriston	38°13'07″	78°50'12″	Potomac River
16	USGS01594000	Little Patuxent River at Savage	39°08'04″	76°48'58″	Patuxent River
17	USGS01582500	Gunpowder Falls at Glencoe	39°32'59″	76°38'10″	Patuxent River
18	USGS01491000	Choptank River near Greensboro	38°59'50″	75°47'09″	Eastern Shore
19	USGS01485000	Pocomoke River near willards	38°23'20″	75°19'28″	Eastern Shore

(JPL) was used in the analysis. Several studies have used the GRACE data, and examples of applications include the evaluation of groundwater depletion (Feng et al., 2013, Girotto et al., 2016; Rodell et al., 2009), the improvement of global hydrological models (Güntner, 2008), the estimation of steric sea-level variations (Lombard et al., 2007), and glacial isostatic adjustment (Steffen et al., 2008). In this analysis, the GRACE TWSC product was used as the reference data for the comparison of the TWSC derived from the various combinations of precipitation, evapotranspiration and runoff products. The GRACE TWS Anomaly (TWSA) products were converted into change in TWS (TWSC) for the above-mentioned study period. The difference between GRACE-observed TWS anomaly (TWSA) for two consecutive time steps shown in Eq. (2) provides the estimates of TWSC.

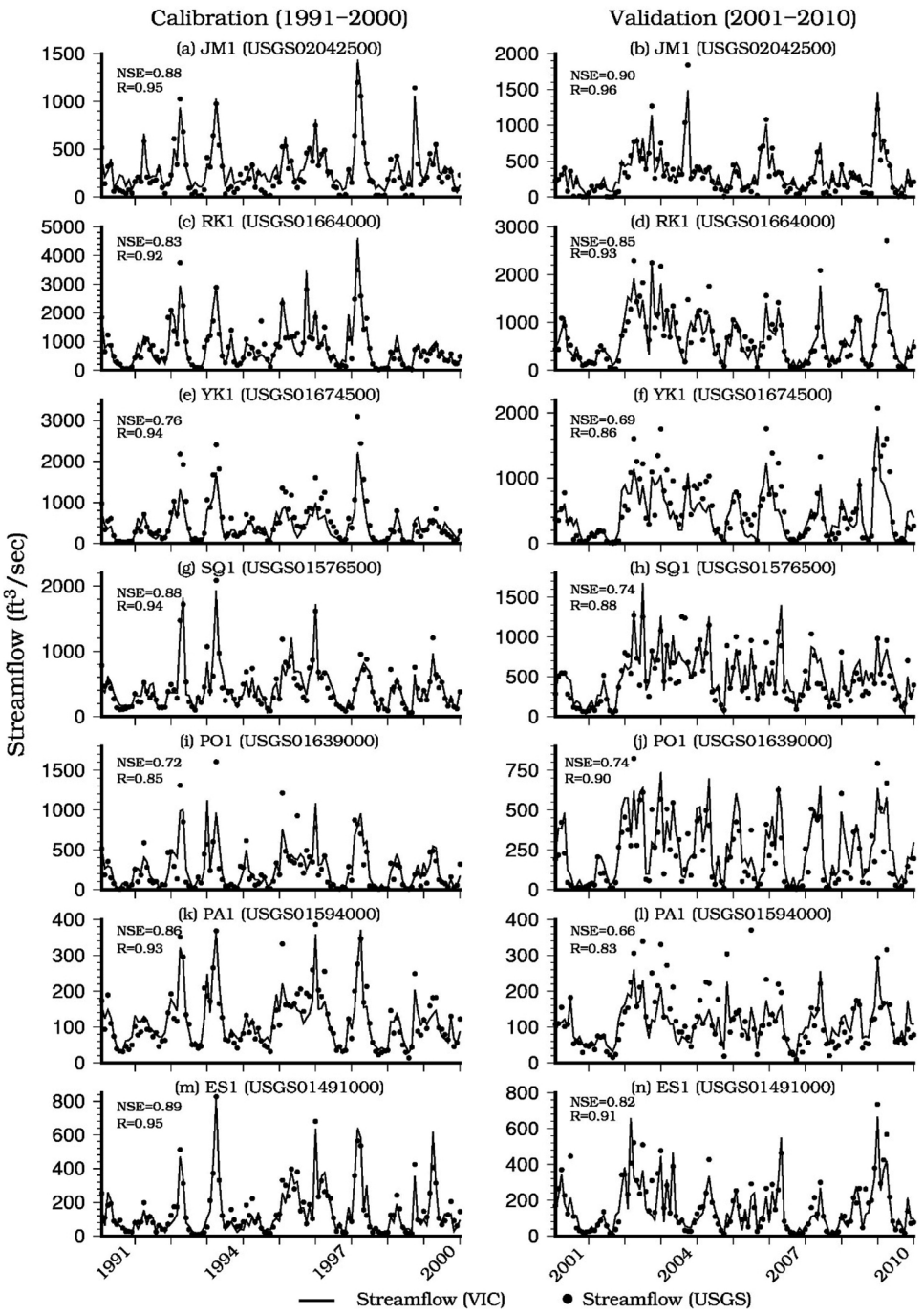

Fig. 4. Calibration (1991–2000) and validation (2001–2010) curve between VIC-simulated streamflow (dashed gray line) and observed USGS streamflow (continuous black line) for 7 stations located in the 7 sub-basins of Chesapeake Bay.

$$TWSC_{GRACE}(\Delta t) = TWSA(t_{i+\Delta t}) - TWSA(t_i) \quad (2)$$

Where $t_{i+\Delta t}$ and t_i represent the ending and starting times, respectively, in the time period Δt. TWSA was converted to TWSC by multiplying the TWSA by the grid scaling factor, as doing so minimized the difference between the smoothed and unfiltered monthly water variations and allowed for consideration of the heterogeneity in the water budget components across the domain (Wiese et al., 2016).

2.4. Hydrologic model

We implemented the VIC model (Liang et al., 1994) for the simulation of streamflow and evapotranspiration in order to calculate the monthly estimates of TWSC. VIC is a large-scale, semi-distributed model that has been used for hydrological predictions and assessment (Jin and Sridhar, 2010; Sridhar et al., 2013; Hokema and Sridhar, 2013), surface and groundwater modeling (Sridhar et al., 2017), drought analysis (Kang and Sridhar, 2017; Kang and Sridhar, 2018; Mishra et al., 2017), climate change impact assessment (Guo et al., 2009), hydropower evaluation (Vicuňa et al., 2011), and determination of anthropogenic effect on water and energy balance simulation (Haddleland et al., 2007). The VIC model solves water and energy fluxes for each grid to enable the estimation of runoff and baseflow. The Arno model conceptualization (Todini, 1996) was used for the calculation of baseflow and excess precipitation-related runoff generation based on the infiltration mechanism outlined in the Xinanjiang model (Ren-Jun, 1992).

The VIC model was implemented at $1/16^{th}$-degree spatial resolution from 1991 to 2016 using monthly time steps for both the calibration and evaluation periods. The meteorological forcing data included precipitation, minimum and maximum temperature, and wind speed. The PRISM-derived daily precipitation, maximum and minimum temperature data; the National Centers for Environmental Prediction; and the National Center for Atmospheric Research (NCEP/NCAR) Reanalysis-based wind data were all used in these simulations. The data were processed using the linear interpolation technique to generate the gridded inputs with a spatial resolution of 1/16th of a degree. The required soil and vegetation data were obtained from the Land Data Assimilation Systems (LDAS) (http://ldas.gsfc.nasa.gov/) at the same spatial resolution as the meteorological data. The soil datasets obtained from LDAS were derived from the 1-km Penn State STATSGO data and contained 11 individual layers up to a depth of 2.5 m and 16 soil texture classifications ranging from sand to bedrock. The VIC model contained three soil layers and were initially set to 0–10 cm, 10–40 cm, and 40–100 cm for the top, middle and deep layers, respectively. We selected the soil layer depths in part due to the model calibration and validation procedure described in the following paragraph. The vegetation parameter file was generated from the LDAS vegetation data, which contained 11 vegetation classes at $1/16^{th}$ of a degree. The routing of the grid-simulated runoff and baseflow was performed using a model developed by Lohmann et al. (1998, 1996), which uses unit hydrograph describing the time travel information of water from each grid to the channel. The linearized Saint Venant's equation guides the routing of flux from each grid through the channel network.

The VIC model parameters used for the calibration include variable infiltration curve (bi_{nf}), maximum baseflow velocity (D_{smax}); fraction of maximum base flow velocity where base flow occurred (D_s); fraction of maximum soil moisture content above which nonlinear base flow occurred (W_s); and top (D1), mid (D2) and deep (D3) soil layer depth (Abdulla and Lettenmaier, 1997a, 1997b; Crow et al., 2003; Troy et al., 2008). D_s and D_{smax} are linked with the control of baseflow, whereas W_s and b_{inf} play a role in the surface runoff. The thickness of the soil layer is associated with the runoff peak and evapotranspiration.

2.4.1. Model calibration and evaluation

The calibration of the VIC model was carried out by comparing the monthly simulated streamflow with the observed USGS streamflow data at 19 gauge stations (Fig. 1, Table 2) during the period 1991–2000. The ability of the VIC model to depict the observed streamflow was quantified by the calculation of Nash–Sutcliffe model efficiency coefficient (NSE, Nash and Sutcliffe, 1970) and correlation coefficient (r) values. The NSE is defined as:

$$\mathrm{NSE} = 1 - \frac{\sum (Q_o^t - Q_m^t)^2}{\sum (Q_o^t - \overline{Q_o})^2} \tag{3}$$

And correlation coefficient (r) is defined as:

$$\mathrm{r} = \frac{n(\sum Q_o^t Q_m^t) - (\sum Q_o^t)(\sum Q_m^t)}{\sqrt{[n\sum (Q_o^t)^2 - (\sum Q_m^t)^2]\,[n\sum (Q_m^t)^2 - (\sum Q_m^t)^2]}} \tag{4}$$

Where $\overline{Q_o}$ is the mean of observed streamflow, Q_o^t is observed streamflow at time t, Q_m^t is modeled streamflow at time t, and n is number of observations.

3. Results and discussion

3.1. Comparisons of MODIS and VIC-simulated evapotranspiration

Evapotranspiration is one of the important components of the water budget, and plays a primary role in the estimation of TWS for this region. Evapotranspiration is dominant in areas covered with forest, due to canopy interception and increased soil moisture with less surface runoff over the ground. Fig. 3 (a–b) shows the spatial distribution of the mean annual evapotranspiration, with values ranging between 50 to 1000 mm over the entire watershed, as simulated by the VIC model and the MODIS-derived product, respectively. The VIC model exhibited a wider range in the simulated evapotranspiration values than the MODIS-derived product, especially in the northern region of the watershed. The Susquehanna and Potomac basins demonstrated some heterogeneity, with simulated evapotranspiration values from 400 mm to 700 mm, and also showed some discrepancies with the MODIS-derived product. The difference in VIC-simulated and MODIS-derived evapotranspiration estimates varied between +300 mm to −300 mm (Fig. 3[c]). The VIC model underestimated the evapotranspiration in large sections of Susquehanna, Potomac, and Patuxent basins when compared with the MODIS values. The overestimation from the VIC-model was minimal, with most of the region showing

values below 150 mm. More than 25% of the watershed showed some differences in evapotranspiration, within ± 50 mm between VIC-simulated and MODIS-derived estimates.

Seasonal variations in evapotranspiration over the Chesapeake Bay watershed and the 7 sub-basins were estimated using the mean monthly values for the same period (Fig. 3 [b, c]). The evapotranspiration was the highest in July, and then decreased until December. The annual cycle of evapotranspiration was mainly governed by temperature variations that closely resembled those in the annual temperature. Evapotranspiration was greater during the growing season (May to August) and decreased as the temperature decreased. The peak of the evapotranspiration during July was higher for the MODIS-derived product when compared with VIC-simulated values, with all 7 sub-basins exhibiting a similar pattern throughout the year. Mean monthly variation in the estimates from the VIC model and the MODIS-derived product showed the underestimation by the VIC model was dominant between June and August (Fig. 3[f]). Clearly, the differences in ET between VIC and MODIS during the peak ET periods suggest that modeling ET is important for TWSC assessment. From Fig. 3f, it is evident that VIC was overestimating ET for the northern and southern portions of the watershed, while central and eastern parts showed underestimations of ET. Due to these overestimations in most areas, especially during drought years, discrepancies in TWSC for the regions including the James, Susquehanna, Patuxent and Eastern Shore sub-watersheds were noticeable. Differences in mean monthly values varied from 15 mm to −25 mm, with standard deviations of ± 13 mm. The overall comparison between them demonstrated the ability of the VIC model to simulate the evapotranspiration more closely, and hence provided the justification for the usefulness of these datasets in estimating TWSC to better understand basin water availability.

3.2. Streamflow analysis

The calibration of the VIC model was performed by comparing simulated and observed monthly streamflow, with the aim of achieving both NSE and *r* values closest to unity. The parameter used in the calibration, the allowable range of values, and the range of the final values of the parameters obtained from the calibration are provided in Table 3. Fig. 4, S1 and S2 show the comparison between the simulated monthly streamflow from the VIC model and the observed streamflow at multiple gauge locations during the calibration period. The NSE and *r*-values obtained for each of the gauge station locations are shown in Table 4. The VIC model was able to simulate the observed streamflow accurately for each of the basins with NSE values for most of the stations greater than 0.7 and *r*-values greater than 0.85 for the period between 1991 and 2000. The VIC model was evaluated using the monthly streamflow observations for the same locations where the model was calibrated, but for the period between 2001 and 2010. The evaluation of the streamflow was found to be satisfactory using the model classification scheme proposed by Moriasi et al. (2007). It should be noted that the validation period for ES2 (USGS01485000) gauge station was discontinuous for two years (2005–2006) when there was no data.

3.3. Estimation of Terrestrial Water Storage Change using the three methods

The hydrological response of the watershed, analyzed using different combinations to estimate TWSC, was presented as the mean monthly values for the period from 2003 to 2016 (Fig. 5). The monthly variations in the PRISM precipitation (Fig. 5a), VIC-simulated evapotranspiration (Fig. 5b), MODIS evapotranspiration (Fig. 5c), VIC-simulated runoff (Fig. 5d), and USGS runoff (Fig. 5e) were used in the combinations specified earlier in order to estimate TWSC. The comparison of the VIC-simulated and MODIS evapotranspiration revealed similar patterns, but the MODIS values were slightly better throughout the study period (Fig. 5b, 5c). However, the monthly VIC-simulated and USGS runoff series were in close agreement (Fig. 5d, 5e).

As mentioned in section 2.2, spatial analysis of TWSC using the three methods was performed with the GRACE-derived TWSC estimates (Fig. 6), and monthly time series (Fig. 7). Fig. 6a shows the mean annual TWSC during 2003–2016, as estimated using the PRISM precipitation, VIC-simulated evapotranspiration, and VIC-simulated runoff. Mean annual estimates of TWSC varied between -30 mm and 30 mm, with the lowest value observed in the James Basin and the highest value in the Eastern Shore, as estimated by the GRACE-derived TWSC. Mean monthly variations in TWSC, using Method 1 with ± 1 standard deviation, are shown in Fig. 7a. The correlation between TWSC estimated using Method 1 and GRACE suggested the overall pattern and magnitudes of change were captured reasonably well over the entire period of 13 years. The mean monthly TWSC using Method 1 varied between −70 mm and 90 mm.

The TWSC calculated using Method 2 (i.e., by replacing the VIC-simulated evapotranspiration in Method 1with the MODIS-

Table 3
Description of the VIC model parameters used for calibration of streamflow.

S. No.	Parameter	Allowable range	Applied value	Unit	Description
1	Ds	0.001 - 1	0.0259 - 0.8888	unitless	Fraction of Dsmax where nonlinear base flow occurs
2	Dsmax	0.1 - 50	0.1254 - 27.7196	mm/d	Maximum baseflow velocity
3	Ws	0 - 1	0.0007 - 0.9748	unitless	Fraction of maximum soil moisture above which nonlinear base flow occurs
4	binf	0.001 - 1	0.0018 - 0.3998	–	Variable infiltration curve parameter
5	D1	0.1 -3	0.1 - 1.4987	m	Top soil layer depth
6	D2	0.1 -3	0.1021 - 1.463	m	Mid soil layer depth
7	D3	0.1 -3	0.1141 - 1.35539	m	Deep soil layer depth

Table 4
Nash-Sutcliffe model efficiency coefficient (NSE) and correlation coefficient (r) values between VIC-simulated streamflow and USGS streamflow for calibration (1990–2000) and validation (2001–2010) periods at USGS station locations.

S. No.	USGS station	Location	Code	Calibration		Validation	
				NSE	r	NSE	r
1	USGS02042500	James River	JM1	0.88	0.95	0.90	0.96
2	USGS02034000	James River	JM2	0.88	0.95	0.83	0.93
3	USGS02024000	James River	JM3	0.92	0.96	0.79	0.89
4	USGS02018000	James River	JM4	0.72	0.85	0.71	0.86
5	USGS02040000	James River	JM5	0.86	0.93	0.84	0.93
6	USGS01664000	Rappahannock River	RK1	0.83	0.92	0.85	0.93
7	USGS01674500	York River	YK1	0.76	0.94	0.69	0.86
8	USGS01671100	York River	YK2	0.72	0.92	0.74	0.88
9	USGS01673550	York River	YK3	0.79	0.90	0.54	0.76
10	USGS01576500	Susquehanna River	SQ1	0.88	0.94	0.74	0.88
11	USGS01534000	Susquehanna River	SQ2	0.78	0.89	0.68	0.88
12	USGS01544000	Susquehanna River	SQ3	0.69	0.87	0.66	0.85
13	USGS01639000	Potomac River	PO1	0.72	0.85	0.74	0.90
14	USGS01601500	Potomac River	PO2	0.58	0.86	0.59	0.85
15	USGS01627500	Potomac River	PO3	0.61	0.82	0.60	0.79
16	USGS01594000	Patuxent River	PA1	0.86	0.93	0.66	0.83
17	USGS01582500	Patuxent River	PA2	0.77	0.89	0.71	0.85
18	USGS01491000	Eastern Shore	ES1	0.89	0.95	0.82	0.91
19	USGS01485000	Eastern Shore	ES2	0.69	0.87	0.59	0.78

derived evapotranspiration) is shown in Fig. 6b. Mean annual TWSC estimates were found to be higher when using Method 2, with a considerable portion of the watershed having values greater than 40 mm or less than -40 mm. Deficit storages from the estimates of TWSC was evident in several sub-basins, including Susquehanna, Potomac, and Patuxent, while other areas of the watershed showed surplus values. Mean annual TWSC for the entire Chesapeake Bay watershed was determined as 6.67 mm using Method 2, as compared to the 0.26 mm estimated from Method 1. Since Method 2 differed from Method 1, with the use of MODIS-derived evapotranspiration instead of VIC-simulated evapotranspiration, the difference was primarily from MODIS data. The spatial patterns of TWSC using Method 2 were similar to the spatial distribution of the difference between VIC- simulated and MODIS-derived evapotranspiration (VIC-simulated minus MODIS-derived evapotranspiration, Fig. 3c). The evapotranspiration values (Fig. 3c, 5 b, 5 c) for the Susquehanna, Potomac, and Patuxent basins were higher with the MODIS-product than the VIC-simulated result, but the TWSC values for these areas were lower when calculated with Method 2 when than the estimates obtained with Method 1. In addition, the TWSC variations calculated using Method 2 were more accurate than those calculated using Method 1 in depicting the GRACE-derived TWSC, with a correlation coefficient value of 0.52 during 2003–2016. Method 2 performed better due to averaging that removed some spikes in the data, resulting in mean monthly TWSC values between -80 mm and 110 mm.

To increase understanding of the role of surface runoff in estimating TWSC, Method 3 was developed by replacing the VIC-simulated runoff in Method 2 with the USGS runoff, so that the components became PRISM precipitation, MODIS-derived evapotranspiration, and USGS runoff. Fig. 6c shows the spatial variation of the mean annual TWSC for the period 2003–2016. There are more regions of deficit evident in Fig. 6c than in Fig. 6b, reflecting the effect of observed streamflow from USGS. Higher deficits were observed in the Susquehanna and Eastern Shore basins, and surplus was evident in the York basin, marking the western half of the Chesapeake Bay watershed as a TWS deficit region. The comparison of the mean monthly VIC-simulated runoff and the USGS runoff showed a similar pattern, but the magnitude of runoff was greater for the USGS data (Fig. 5d, e). The inclusion of the higher runoff value in Eq. (1) caused the model to show a TWSC deficit over several regions within the watershed. Even though the area with the TWS deficit expanded, the intensity of the TWS deficiency decreased, resulting in an average annual TWSC of 14.2 mm for the Chesapeake Bay watershed. Fig. 7c shows the mean monthly variation in TWSC for the watershed from 2003 to 2016. Method 3 was able to capture TWSC reasonably well; however, the correlation coefficient between the TWSC simulated using this method and the GRACE-derived TWSC was 0.45, which was least among the three methods.

The magnitudes of GRACE-derived annual TWSC varied spatially, with the lowest value of −10 mm occurring over the James River Basin, while the highest values were present mostly in the Eastern Shore Basin (Fig. 6[d]). Fig. 7 (bar plots) shows the monthly variation of GRACE-derived TWSC for the Chesapeake Bay watershed from 2003 to 2016, with values ranging from −100 mm to 95 mm. GRACE-derived TWS estimates showed deficit storage between June and September, while the remaining months were marked with surpluses. Seasonal variations in TWSC suggested that seasonal temperatures had opposite effects on TWSC (Fig S3). The region is typically warmer in the months between June and September, and cooler during the other months. The variation in TWSC explained these characteristics. It can be suggested that TWSC dynamics appeared to be governed primarily by temperature and precipitation anomalies.

3.4. Terrestrial water storage change for drought and non-drought years

Terrestrial Water Storage Change has been used for the evaluation of drought in various countries, including the US (Jin and

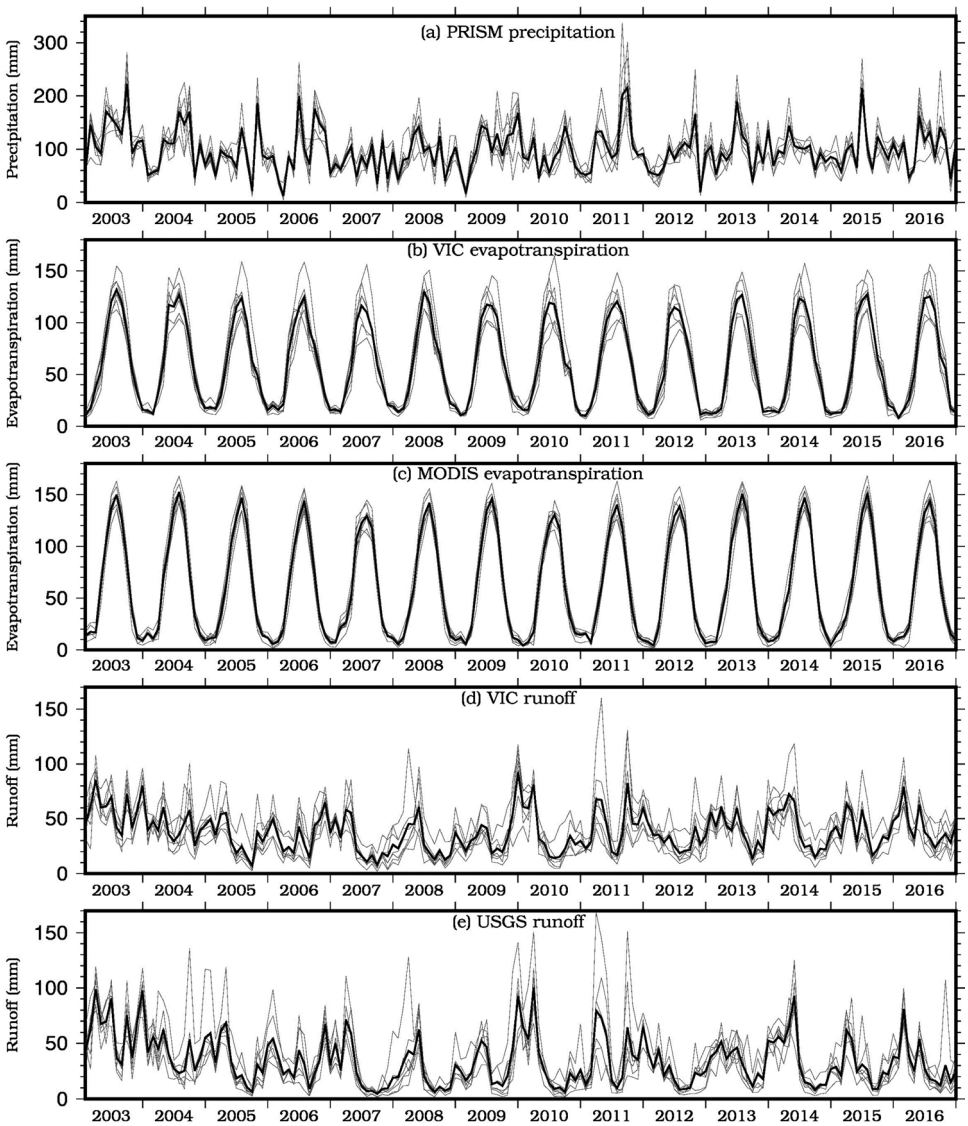

Fig. 5. Monthly variation in PRISM precipitation (mm/month), VIC-simulated evapotranspiration (mm/month), MODIS evapotranspiration (mm/month), VIC-simulated runoff (mm/month), and USGS runoff (mm/month) for 7 sub-basins (gray line) and Chesapeake Bay (black line) for.2003–2016.

Zhang, 2016), India (Sinha et al., 2017), and China (Sun et al., 2018). While the average or normal year in terms of climatology or hydrology can be useful in understanding how GRACE data can help in mapping water availability over large areas, it can also be effective for water management during drought and non-drought years. In order to investigate its utility, an additional assessment was performed using the data generated from Method 1 and compared with the estimates of GRACE-derived TWSC. The period of the drought in the Chesapeake Bay watershed from 2003 to 2016 was adopted from the study performed by Kang and Sridhar (2018), which involved identifying moderate to extreme drought condition events using precipitation and the Palmer Drought Severity Index (PDSI). A total of four years—2007, 2008, 2010, and 2012—were used for the drought period, while the remaining years were categorized as non-drought years.

Method 1 was employed to estimate TWSC for both drought and non-drought years using PRISM precipitation, VIC-simulated evapotranspiration, and VIC-simulated runoff data. Fig. 8a shows the spatial distribution of the mean annual TWSC during the non-drought period. The mean annual TWS remained relatively high for most of the watershed area, with an average value of 13.2 mm. TWSC estimates within the Susquehanna Basin were negative, while the highest value of TWSC, over 80 mm, was evident in the Potomac and Eastern Shore basins. Deficits in TWS for the drought period were evident in the area with a mean annual TWSC of -32 mm (Fig. 8b). The region with the lowest TWSC included the James Basin, along with some areas of the Potomac, York and Eastern Shore basins. As well, a considerable portion of the Susquehanna Basin exhibited surpluses, with TWSC estimates up to 40 mm. The difference between the TWSC for the drought period and that for the non-drought period highlighted the impact of

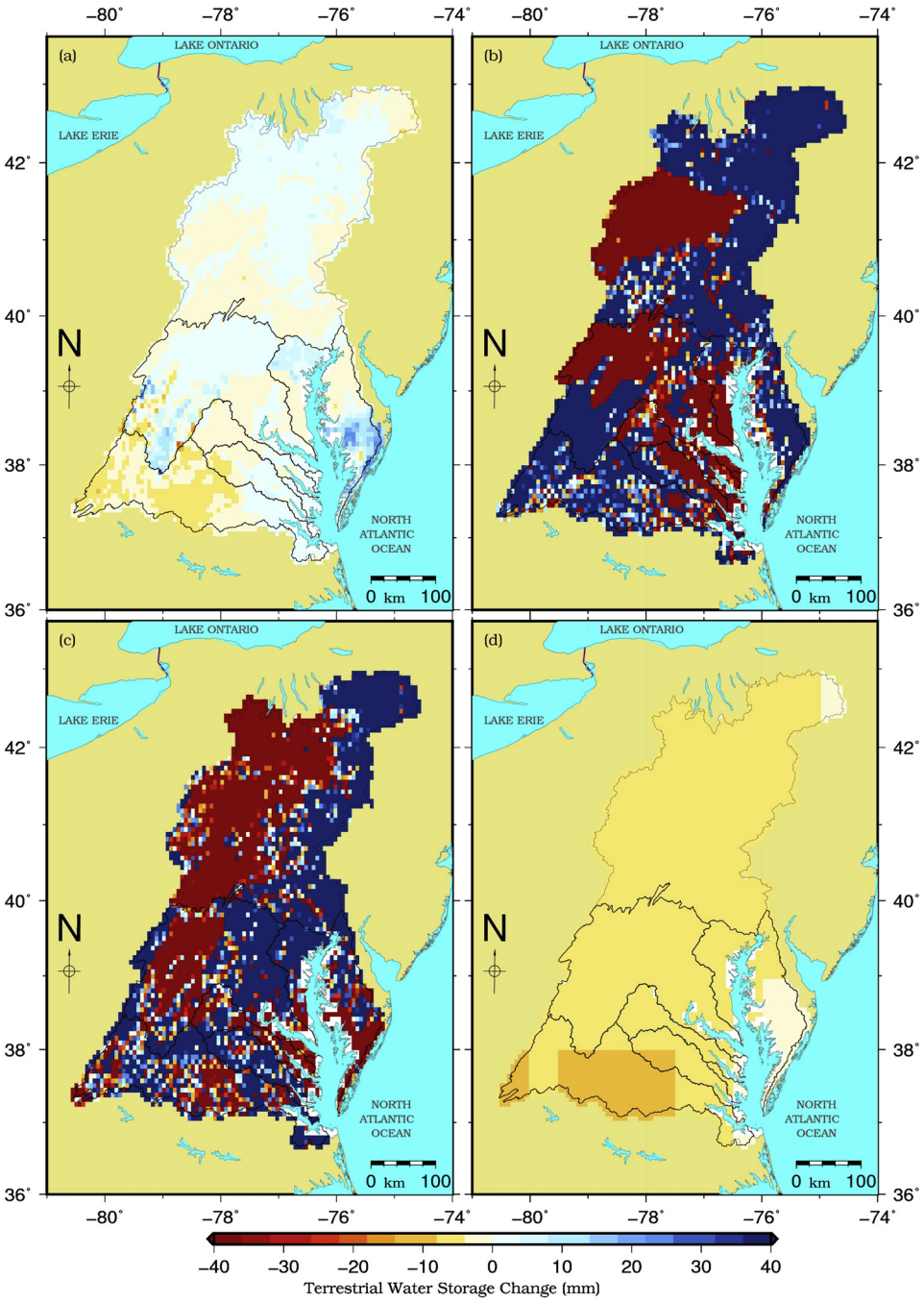

Fig. 6. Annual Terrestrial Water Storage Change (TWSC, mm) for Chesapeake Bay using (a) Method 1 (PRISM precipitation, VIC-simulated Evapotranspiration, and VIC-simulated runoff), (b) Method 2 (PRISM precipitation, MODIS Evapotranspiration, and VIC-simulated runoff), (c) Method 3 (PRISM precipitation, MODIS Evapotranspiration, and USGS runoff), and (d) GRACE for.2003–2016.

drought as shown in Fig. 8c. Although the drought had an effect on the entire Chesapeake Bay watershed, the severity was obvious in the James and the Eastern Shore, Potomac, York, Patuxent and Susquehanna River basins. Since the classification of the years into drought and non-drought periods was based on precipitation, the spatial variation in precipitation over the region influenced the heterogeneous response of the different basins. Monthly variations in PRISM precipitation (Fig. 5a), VIC-simulated evapotranspiration (Fig. 5b), and VIC-simulated runoff (Fig. 5d) explained the deficit in TWS during the drought period. Similar patterns were seen in the monthly variations of the VIC-simulated evapotranspiration between 2003 and 2016. However, VIC-simulated runoff had no discernable pattern during the drought years. Perhaps the PRISM precipitation was lower in the drought period (2007, 2008, 2010, and 2012) than in other years, resulting in the deficit TWS during these years.

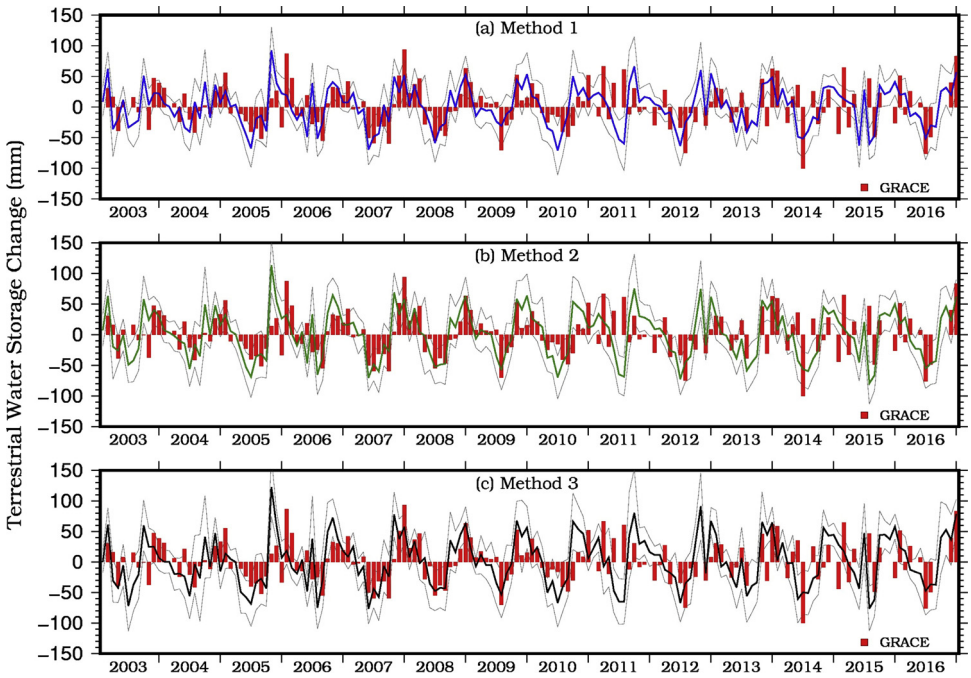

Fig. 7. Comparison of monthly variation of Terrestrial Water Storage Change (TWSC, mm/month) between (a) Method 1 (PRISM precipitation, VIC-simulated Evapotranspiration, and VIC-simulated runoff), (b) Method 2 (PRISM precipitation, MODIS Evapotranspiration, and VIC-simulated runoff), (c) Method 3 (PRISM precipitation, MODIS Evapotranspiration, and USGS runoff), and (d) GRACE (red bars) along with the uncertainty (± 1 standard deviation) for.2003–2016.

Fig. 8d shows the mean monthly variations in TWSC for the entire Chesapeake Bay watershed during the drought and non-drought periods, as estimated using Method 1. Fig. 9 shows the results for each sub-basin in the watershed. The TWSC variation between the drought and non-drought periods remained similar for most months during the year, but the contrast was obvious from May to July. Besides the negative values of TWSC during both drought and non-drought period, TWSC during the drought period was lower than -40 mm, and reached its minimum in June. On the other hand, the TWSC for the non-drought months, May to July, remained greater than -40 mm. The difference in the estimated TWSC during the non-drought and drought periods was also the highest in June, at 40 mm. Fig. 8e shows the mean monthly TWSC estimated using the GRACE product, which remained lower during the drought periods for the Chesapeake Bay watershed. However, the difference between the drought and non-drought periods varied widely over the year and by each sub-basin, causing some challenges in determining a threshold value of TWSC by which to distinguish the responses between them. As is evident from Fig. 9a, Method-1-based TWSC estimates were very close to GRACE for each sub-basin and the entire watershed. From Fig. 9b, it is clear that the Eastern Shore, York and James basins showed big differences between GRACE and TWSC estimates obtained with Method 1. It can be suggested that in these sub-basins, where streamflows and land cover are managed, TWSC estimates that do not consider anthropogenic factors can introduce some uncertainties.

4. Conclusions

This study emphasizes the use of satellite, in-situ and simulation data for assessing the hydrologic budget and water availability in the Chesapeake Bay watershed. The investigation offered insights into employing observed streamflow to calibrate VIC, thus providing better streamflow estimates, and ultimately ET. This, in combination with PRISM precipitation data and VIC-simulated ET or MODIS-derived ET, enhanced TWSC predictions for the watershed. It was also noted that predicting ET is critical for TWSC, especially from June to August, and that VIC-simulated TWSC could be a reliable proxy for GRACE data in the assessment of water availability. Major portions of the region exhibited water excess conditions; however, the James River basin was marked with deficits in storage. The mean annual TWSC varied from +30 mm to -30 mm, but the monthly values fluctuated between −70 mm and 90 mm, with deficits occurring between June and September, while the remaining months were identified to have higher storage levels than TWS estimates indicated.

The anthropogenic effect was not considered in this analysis, but can play a major role in altering the estimates of TWSC over the study area. Therefore, future studies can focus on anthropogenic impacts, with long-term simulations and forecasts using better climate forcing to predict the water resources for this climatologically-sensitive region in the United States. The assessment of water resources in a heterogeneous region also warrants the use of multiple sources of data, such as in-situ, satellite-based and hydrological model-simulated states and fluxes, when available.

When high-resolution information is needed for decision-making at the watershed scale, VIC-simulated TWSC data can reliably fill

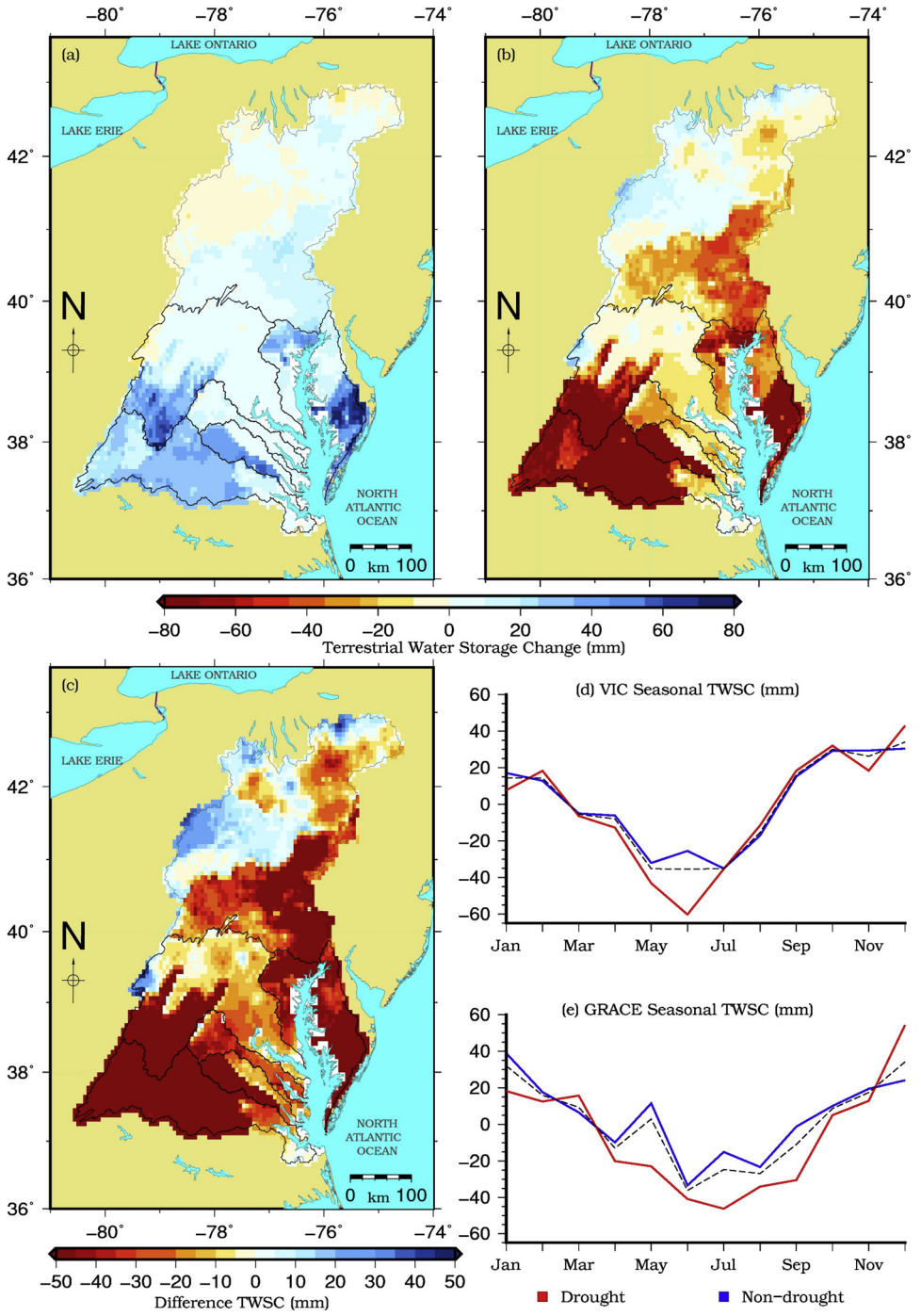

Fig. 8. Terrestrial Water Storage Change analysis during non-drought period and drought period. (a) Mean annual TWSC (mm) during the non-drought period, (b) mean annual TWSC (mm) during the drought period, (c) TWSC difference (drought TWSC minus non-drought TWSC) between dorught and non-drought period. (d) Seasonal variation of TWSC (mm/month) during drought period (red), non-drought period (blue), and normal period (dashed black line) from VIC model, and (e) GRACE product.

gaps in time and space. This is especially true when localized extreme events such as meteorological or hydrological droughts occur, and VIC-derived TWSC can be provided as forecasts with proper state variables, including environmental, vegetation and soil moisture conditions. The southern region of the Chesapeake Bay watershed and Eastern Shore were identified as more drought-prone, and they can be effectively monitored by a combination of VIC and GRACE estimates of TWSC during May–July since a single-source assessment of water resource availability and drought can lead to uncertainties.

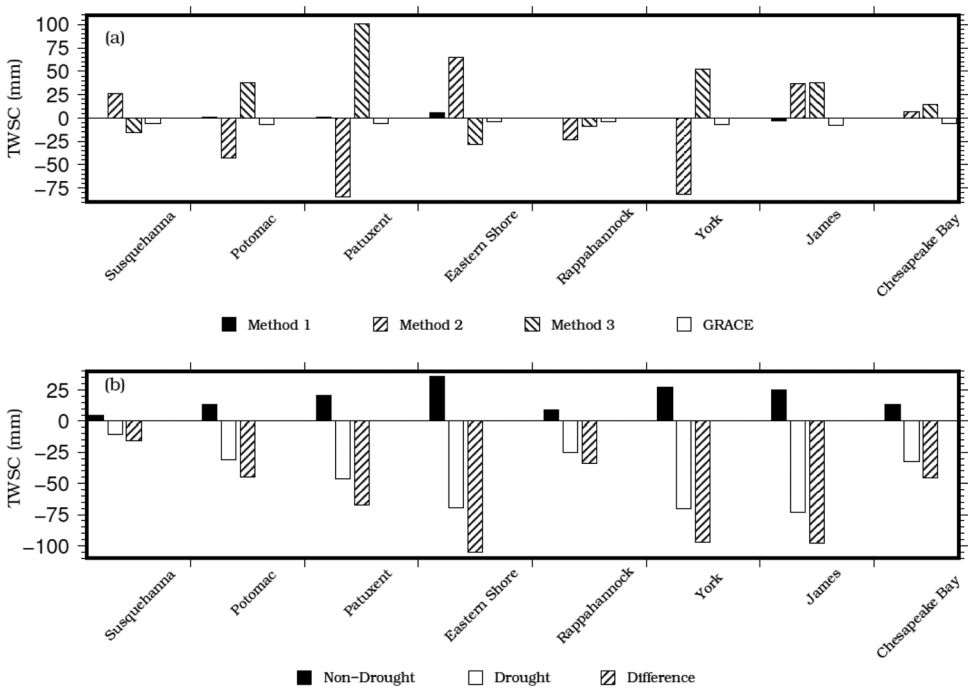

Fig. 9. Terrestrial Water Storage Change analysis for each sub-basin in the Chesapeake Bay using (a) Method 1 (PRISM precipitation, VIC-simulated Evapotranspiration, and VIC-simulated runoff), Method 2 (PRISM precipitation, MODIS Evapotranspiration, and VIC-simulated runoff), and Method 3 (PRISM precipitation, MODIS Evapotranspiration, and USGS runoff) for 2003–2016. (b) Comparisons of TWSC between VIC using Method 1 and GRACE for each basin during drought and non-drought periods.

Declaration of interests

None.

Acknowledgements

This project was funded in part by the Virginia Agricultural Experiment Station (Blacksburg) and the Hatch Program of the National Institute of Food and Agriculture, U.S. Department of Agriculture (Washington, D.C.).

Appendix A. Supplementary data

Supplementary material related to this article can be found, in the online version, at doi:https://doi.org/10.1016/j.ejrh.2019.100607.

References

Abdulla, F.A., Lettenmaier, D.P., 1997a. Development of regional parameter estimation equations for a macroscale hydrologic model. J. Hydrol. 197, 230–257. https://doi.org/10.1016/S0022-1694(96)03262-3.

Abdulla, F.A., Lettenmaier, D.P., 1997b. Application of regional parameter estimation schemes to simulate the water balance of a large continental river. J. Hydrol. 197, 258–285. https://doi.org/10.1016/S0022-1694(96)03263-5.

Berbery, E.H., Luo, Y., Mitchell, K.E., Betts, A.K., 2003. Eta model estimated land surface processes and the hydrologic cycle of the Mississippi basin. J. Geophys. Res.-Atmos. 108 doi:10/1029/2002JD003192.

Billah, M.M., Goodall, J.L., 2011. Annual and interannual variations in terrestrial water storage during and following a period of drought in South Carolina, USA. J. Hydrol. 409. https://doi.org/10.1016/j.jhydrol.2011.08.045.

Billah, M.M., Goodall, J.L., Narayan, U., Reager, J.T., Lakshmi, V., Famiglietti, J.S., 2015. A methodology for evaluating evapotranspiration estimates at the watershed-scale using GRACE. J. Hydrol. 523, 574–586. https://doi.org/10.1016/j.jhydrol.2015.01.066.

Crow, W.T., Wood, E.F., Pan, M., 2003. Multiobjective calibration of land surface model evapotranspiration predictions using streamflow observations and spaceborne surface radiometric temperature retrievals. J. Geophys. Res. 108. https://doi.org/10.1029/2002JD003292.

Daly, C., Neilson, R.P., Phillips, D.L., 1994. A statistical-topographic model for mapping climatological precipitation over mountainous terrain. J. Appl. Meteorol. Climatol. 33 (2), 140–158. https://doi.org/10.1175/1520-0450(1994)033<0140:ASTMFM>2.0.CO;2.

Gao, H., Tang, Q., Ferguson, C.R., Wood, E.F., Lettenmaier, D.P., 2010. Estimating the water budget of major US river basins via remote sensing. Int. J. Remote Sens. 31 (14), 3955–3978. https://doi.org/10.1080/01431161.2010.483488.

Gibson, W.P., Daly, C., Kittel, T., Nychka, D., Johns, C., Rosenbloom, N., McNab, A., Taylor, G., 2002. Development of a 103-year high-resolution climate data set for the conterminous United States. 13th AMS Conference on Applied Climatology. Am. Meteorol. Soc. 181–183.

Girotto, M., De Lannoy, G.J., Reichle, R.H., Rodell, M., 2016. Assimilation of gridded terrestrial water storage observations from GRACE into a Land Surface Model.

Water Resour. Res. 52, 4164–4183. https://doi.org/10.1002/2015WR018417.
Haddleland, I., Skaugen, T., Lettenmaier, D.P., 2007. Hydrologic effects of land and water management in North America and Asia: 1700–1992. Hydrol. Earth Syst. Sci. Discuss. 11, 1035–1045. https://hal.archives-ouvertes.fr/hal-00305067.
Hanasaki, N., Kanae, S., Oki, T., 2006. A reservoir operation scheme for global river routing models. J. Hydrol. 327, 22–41. https://doi.org/10.1016/j.jhydrol.2005.11.011.
Hoekema, D.J., Sridhar, V., 2013. A system dynamics model for conjunctive management of water resources in the Snake River Basin. J. Am. Water Resour. As. 49 (6), 1327–1350. https://doi.org/10.1111/jawr.12092.
Lakshmi, V., 2016. Beyond GRACE: using satellite data for groundwater investigations. Groundwater 54 (5), 615–618. https://doi.org/10.1111/gwat.12444.
Luo, Y., Berbery, E.H., Mitchell, K.E., 2005. The operational eta model precipitation and surface hydrologic cycle of the Columbia and Colorado basins. J. Hydrometeorol. 6, 341–370. https://doi.org/10.1175/JHM435.1.
Mccabe, M.F., Wood, E.F., Wojcik, R., Pan, M., Sheffield, J., Gao, H., Su, H., 2008. Hydrological consistency using multi-sensor remote sensing data for water and energy cycle studies. Remote Sens. Environ. 112, 430–444. https://doi.org/10.1016/j.rse.2007.03.027.
Mu, Q., Heinsch, F.A., Zhao, M., Running, S.W., 2007. Development of a global evapotranspiration algorithm based on MODIS and global meteorology data. Remote Sens. Environ. 111, 519–536. https://doi.org/10.1016/j.rse.2007.04.015.
Mu, Q., Zhao, M., Running, S.W., 2011. Improvements to a MODIS global terrestrial evapotranspiration algorithm. Remote Sens. Environ. 115, 1781–1800. https://doi.org/10.1016/j.rse.2011.02.019.
Nash, J.E., Sutcliffe, J.V., 1970. River flow forecasting through conceptual models part I—a discussion of principles. J. Hydrol. 10, 282–290. https://doi.org/10.1016/0022-1694(70)90255-6.
Nilsson, C., Reidy, C.A., Dynesius, M., Revenga, C., 2005. Fragmentation and flow regulation of the world's large river systems. Science 308, 405–408. https://doi.org/10.1126/science.1107887.
Oki, T., Kanae, S., 2006. Global hydrological cycles and world water resources. Science 313, 1068–1072. https://doi.org/10.1126/science.1128845.
Rodell, M., Famiglietti, J.S., 2001. An analysis of terrestrial water storage variations in Illinois with implications for the Gravity Recovery and Climate Experiment (GRACE). Water Resour. Res. 37 (5), 1327–1339. https://doi.org/10.1029/2000WR900306.
Rodell, M., Famiglietti, J.S., Chen, J., Seneviratne, S.I., Viterbo, P., Holl, S., Wilson, C.R., 2004. Basin scale estimates of evapotranspiration using GRACE and other observations. Geophys. Res. Lett. 31, L20504. https://doi.org/10.1029/2004GL020873.
Rodell, M., Velicogna, I., Famiglietti, J., 2009. Satellite data show Indian water stocks shrinking. Nature 460 (7257). https://doi.org/10.1038/460789a. 789-789.
Seong, C., Sridhar, V., 2017. Hydroclimatic variability and change in the Chesapeake Bay Watershed. J. Water Clim. Change 8 (2), 254–273. https://doi.org/10.2166/wcc.2016.008.
Seong, C., Sridhar, V., Billah, M.M., 2017. Implications of potential evapotranspiration methods for streamflow estimation in a changing climate. Int. J. Climatol. 38 (2), 896–914. https://doi.org/10.1002/joc.5218.
Sheffield, J., Ferguson, C.R., Troy, T.J., Wood, E.F., Mccabe, M.F., 2009. Closing the terrestrial water budget from satellite remote sensing. Geophys. Res. Lett. 36, L07403 doi:07410.01029/02009GL037338.
Sridhar, V., 2013. Tracking the influence of irrigation on land surface fluxes and boundary layer climatology. J. Cont. Water Res. Educ. 152 (1), 79–93. https://doi.org/10.1111/j.1936-704X.2013.03170.x.
Sridhar, V., Jaksa, W.T.A., Fang, B., Lakshmi, V., Hubbard, K.G., Jin, X., 2013. Evaluating bias corrected AMSR-E soil moisture using in-situ observations and model estimates. Vadose Zone J. https://doi.org/10.2136/vzj2013.05.0093.
Sridhar, V., Hubbard, K.G., Wedin, D.A., 2006. Assessment of soil moisture dynamics of the Nebraska Sandhills using long-term measurements and a hydrology model. J. Irrig. Drain. Eng. 132 (5), 463–473. https://doi.org/10.1061/(ASCE)0733-9437(2006)132:5(463).
Sridhar, V., Wedin, D.A., 2009. Hydrological behaviour of grasslands of the Sandhills of Nebraska: water and energy-balance assessment from measurements, treatments, and modelling. Ecohydrology 2, 195–212. https://doi.org/10.1002/eco.61.
Su, F.G., Lettenmaier, D.P., 2009. Estimation of the surface water budget of La Plata Basin. J. Hydrometeorol. 10, 981–998. https://doi.org/10.1175/2009JHM1100.1.
Tang, Q.H., Gao, H.L., Lu, H., Lettenmaier, D.P., 2009. Remote sensing: hydrology. Prog. Phys. Geog. 33, 490–509. https://doi.org/10.1177/0309133309346650.
Tang, Q.H., Gao, H.L., Yeh, P., Oki, T., Su, F., Lettenmaier, D.P., 2010. Dynamics of terrestrial water storage change from observations and modeling. J. Hydrometeorol. 11, 156–170. https://doi.org/10.1080/01431161.2010.483488.
Thilakarathne, M., Sridhar, V., 2017. Characterization of future drought conditions in the Lower Mekong River Basin. Weather Clim. Extre. 17, 47–58. https://doi.org/10.1016/j.wace.2017.07.004. http://hdl.handle.net/10919/84334.
Troy, T.J., Wood, E.F., Sheffield, J., 2008. An efficient calibration method for continental-scale land surface modeling. Water Resour. Res. 44. https://doi.org/10.1029/2007WR006513.
USEPA (United States Environmental Protection Agency), 2010. Chesapeake Bay Phase 5.3 Community Watershed Model. EPA 903S10002 - CBP/TRS-303-10. U.S.
USGS (United States Geological Survey), 2016. National Water Information System Data Available on the World Wide Web (USGS Water Data for the Nation). accessed (June 10, 2012), at URL. http://waterdata.usgs.gov/nwis/.